# Anderson disorder in graphene nanoribbons: A local distribution approach

Gerald Schubert,[1,2] Jens Schleede,[1] and Holger Fehske[1]
[1]*Institut für Physik, Ernst-Moritz-Arndt Universität Greifswald, 17487 Greifswald, Germany*
[2]*Regionales Rechenzentrum Erlangen, 91058 Erlangen, Germany*
(Received 7 April 2009; revised manuscript received 14 May 2009; published 9 June 2009)

Disorder effects strongly influence the transport properties of graphene-based nanodevices even to the point of Anderson localization. Focusing on the local density of states and its distribution function, we analyze the localization properties of actual size graphene nanoribbons. In particular, we determine the time evolution and localization length of the single-particle wave function in dependence on the ribbon extension and edge geometry as well as on the disorder type and strength.

DOI: 10.1103/PhysRevB.79.235116 PACS number(s): 73.20.Fz, 05.60.Gg, 71.30.+h, 72.15.Rn

## I. INTRODUCTION

Disorder effects in graphene are of particular importance on the account of its two-dimensional (2D) lattice structure. The single-parameter scaling theory predicts that in 2D systems, arbitrary weak disorder leads to Anderson localization of the single-particle wave function.[1] For graphene, it has been argued that due to the linear dispersion in the vicinity of the band center the one-parameter scaling theory does not hold. The problem of Anderson localization in graphene is therefore heavily debated.[2–4]

Accessing Anderson localization both theoretically and experimentally, the local density of states (LDOS) is a central quantity. By means of the local distribution approach, the distribution of the LDOS may be used to distinguish localized from extended states.[5–7] Nowadays, the LDOS can be directly measured by scanning tunneling spectroscopy experiments.[8–11]

An ordered infinite graphene sheet is a zero-gap semiconductor with a linear density of states near the charge neutrality point.[12] Cutting a graphene nanoribbon (GNR) of finite width out of such a sheet, additional aspects have to be considered. First, the finite number of transverse atoms causes quantum confinement, where the presence of the edges leads to a symmetry breaking. Second, lattice defects or targeted implementations of, e.g., boron ($B_7$) clusters,[13] result in random samples. Thereby, the range of the disorder is of great importance.[14] For long-range disorder, as caused by ripples in the graphene sheet, the two independent corners of the Brillouin zone are untangled and long-wavelength excitations can be modeled by an effective Dirac equation. If the scattering potential is short ranged, however, intervalley scattering between the two inequivalent Dirac cones becomes possible. Third, the finite extension (aspect ratio) of the GNR introduces a new length scale being absent in infinite graphene sheets. Actually, we expect metallic behavior of disordered quasi-one-dimensional (quasi-1D) GNRs if the localization length becomes comparable or even larger than the longitudinal ribbon size.[15–17]

To address these questions, in this work we investigate the electronic structure and the localization properties of disordered GNRs by means of unbiased numerical techniques. Thereby, we focus on the interplay of disorder, boundaries effects, and GNR geometry. Particular aspects of various kinds of disorder in GNRs have been investigated previously in the literature.[15–22]

## II. MODEL AND METHODS

To this end, we consider the tight-binding Hamiltonian

$$H = \sum_{i=1}^{N} \epsilon_i c_i^\dagger c_i - t \sum_{\langle ij \rangle} (c_i^\dagger c_j + \text{H.c.}) \tag{1}$$

on a honeycomb lattice with $N$ sites, including hopping between nearest neighbors $\langle ij \rangle$ only. Drawing the on-site potentials $\epsilon_i$ from the box distribution

$$p[\epsilon_i] = \frac{1}{\gamma} \theta(\gamma/2 - |\epsilon_i|), \tag{2}$$

we introduce (short-ranged) Anderson disorder.[23] We distinguish between bulk ($\gamma_b$) and edge ($\gamma_e$) disorder, when all on-site potentials are subjected to $p[\epsilon_i]$ or only those at the edge sites. We consider quasi-1D GNRs of finite widths with open (periodic) boundary conditions in transverse (longitudinal) direction. Depending on the orientation of the GNRs with respect to the honeycomb lattice, zigzag or armchair geometries will be realized (see panels on top of Fig. 1).

The local properties of site $i$ of a sample with broken translational invariance are reflected in the LDOS,

$$\rho_i(E) = \sum_{m=1}^{N} |\langle i|m\rangle|^2 \delta(E - E_m). \tag{3}$$

Recording the probability density function $f[\rho_i]$ for many different sites $\{i\}$ of a given sample and different sample realizations $\{\epsilon_i\}$ restores the translational invariance on the level of distributions. The shape of $f[\rho_i]$ is determined by $p[\epsilon_i]$ but independent of $\{i\}$ and $\{\epsilon_i\}$.[7] For extended states, $f[\rho_i]$ is strongly peaked around the mean DOS,

$$\rho_{\text{me}} = \langle \rho_i \rangle, \tag{4}$$

independent of the system size; whereas for localized states $f[\rho_i]$ exhibits a log-normal distribution that becomes singular for increasing system sizes.[24] Normalizing the LDOS to $\rho_{\text{me}}$ allows for a detection of the localization properties by performing a finite-size scaling for the LDOS distribution. More conveniently, the typical DOS

 

$$\rho_{\mathrm{ty}} = e^{\langle \ln \rho_i \rangle} \tag{5}$$

monitors the changes in the LDOS distribution. While for $N \to \infty$ an extended state is characterized by finite values of $\rho_{\mathrm{me}}$ and $\rho_{\mathrm{ty}}$, for localized states $\rho_{\mathrm{me}}$ is finite but $\rho_{\mathrm{ty}} \to 0$.[24]

Alternatively, the recurrence probability $P_R(t \to \infty)$ also reveals the localization properties of the system.[25] While in the thermodynamic limit $P_R \sim 1/N \to 0$ for extended states, localized states are characterized by a finite value of $P_R$. Starting from a localized wave packet, we are able to calculate the time-dependent local particle density,

$$n_i(t) = |\psi(\mathbf{r}_i, t)|^2 = \left| \sum_{m=1}^{N} e^{-\mathrm{i}E_m t} \langle m | \psi(0) \rangle \langle i | m \rangle \right|^2, \tag{6}$$

by expanding the time evolution operator into a finite series of Chebyshev polynomials.[26,27] The above local distribution approach also applies to $n_i(t)$. But since an initial state in general contains contributions of the whole spectrum, examining $n_i(t)$ does not allow for an energy-resolved investigation of localization as by the LDOS. Instead it provides a tool for a global examination of the spectrum with relevance for possible measurements. Note that a finite overlap of just one extended state with the initial state leads to a complete spreading of this state after some time.

## III. NUMERICAL RESULTS

### A. Local density of states

Compared to the band structure of an infinite 2D graphene sheet, the DOS of finite GNRs is characterized by a multitude of Van Hove singularities (see top panels of Fig. 1). For zigzag GNRs, the strong signature at $E=0$ indicates the high degeneracy of the edge states.[28] In contrast, armchair GNRs with $N_a=3n$ or $N_a=3n+1$ are gapped around $E=0$. This finite-size gap tends to zero as $N_a \to \infty$. The resulting metallicity for $N_a=3n+2$ is an artifact of the nearest-neighbor (NN) tight-binding approximation, however, and vanishes if next NN and third NN are taken into account.[29] For other values of $N_a$, a longer-ranged hopping slightly modifies the gap size but does not change the fundamental behavior. Note that even for vanishing Anderson disorder the LDOS varies for different bulk sites according to their relative position to the ribbon edges. Symmetry considerations show that there are $N_z$ ($N_a/2$) inequivalent lattice sites in ordered zigzag and armchair GNRs. Therefore, mean and typical DOS do not coincide even for $\gamma_b=0$ (see, e.g., the band center of the zigzag GNR).

If disorder comes in, localized states emerge in the band gap of the armchair GNRs, and above a critical disorder strength the gap is filled completely. The localization properties of the states can readily be seen from the system size dependence of $\rho_{\mathrm{ty}}$. A tendency toward reduced values of $\rho_{\mathrm{ty}}$ for increasing system sizes indicates localization for both GNR geometries and all energies. While this localization effect arises for bulk disorder already at $\gamma_b/\bar{t}=2$, an edge disorder strength of $\gamma_e/\bar{t}=2$ is still too weak to localize the wave function on GNRs of $L=213$ nm size as indicated by the approximate equality of $\rho_{\mathrm{ty}}$ and $\rho_{\mathrm{me}}$. A substantial reduction of $\rho_{\mathrm{ty}}$ is only observed for larger systems ($L=1064$ nm) which indicates localization on a larger length scale. Obviously, zigzag GNRs are less sensible to edge disorder than armchair GNRs since this geometry has only half the number of (disordered) edge sites. The different edge geometries are only of importance if the disorder is weak. For strong disorder $\gamma_b/\bar{t}=4$, the results for armchair and zigzag GNRs coincide almost exactly.

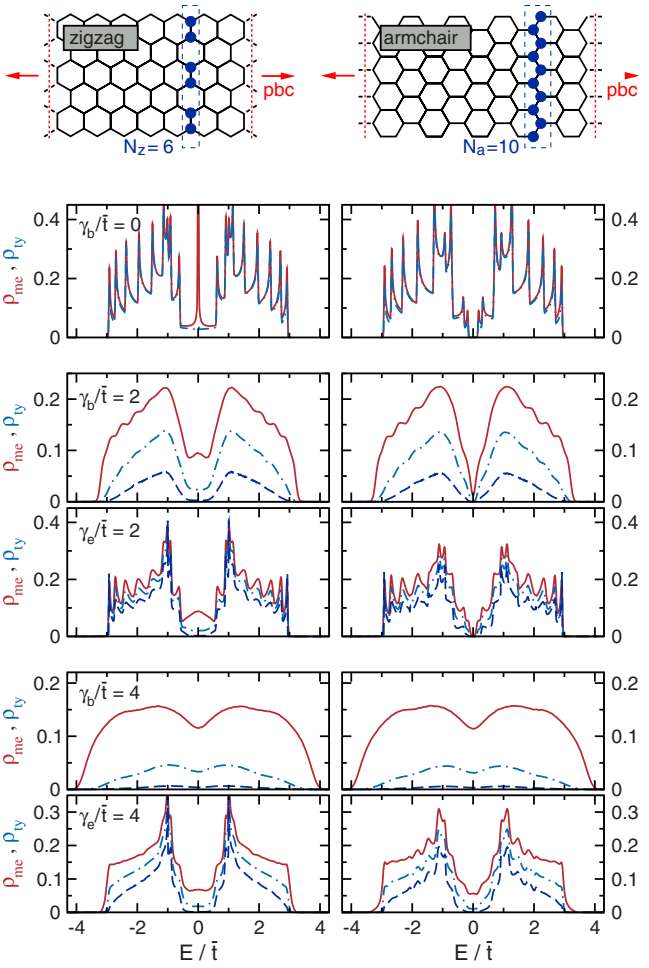


FIG. 1. (Color online) Mean (solid red) and typical (dashed blue) DOS for zigzag (left column, $N_z=6$) and armchair (right column, $N_a=10$) GNRs of width $W=1.1$ nm. Top panels: ordered case. Lower panels: in each $(2\times2)$ block, we compare for a fixed value of disorder the influence of bulk disorder ($\gamma_b$, upper rows) to edge disorder ($\gamma_e$, bottom rows). To illustrate the localization properties, in each panel $\rho_{\mathrm{ty}}$ is given for $L=213(1064)$ nm by light blue dot-dashed (dark blue dashed) lines. These system sizes correspond to 10 000 (50 000) lattice sites for the armchair and 10 392 (51 960) for the zigzag case. Disorder averaging was performed over $10^5$ realizations. In the longitudinal direction, periodic boundary conditions (pbc) are applied.

As stressed above, there are three branches of gap sizes depending on $\mathrm{mod}(N_a,3)$. In Fig. 2, we focus on $N_a=3n+1$ and examine the influence of both bulk and edge disorder on the gap size $\Delta_a$ in dependence on the ribbon width. For our finite system we calculate $\Delta_a$ as

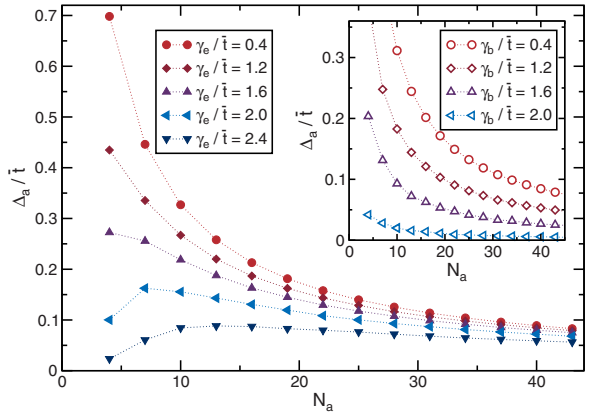


FIG. 2. (Color online) Gap size $\Delta_a$ for armchair GNRs as a function of ribbon width $N_a=3n+1$ for edge disorder (main panel) and bulk disorder (inset). Results are based on the averaged DOS for GNRs with a length of 1000 atoms using 4096 realizations of disorder.

$$\int_{-\Delta_a/2}^{\Delta_a/2} \rho_{\mathrm{me}}(E)dE = \frac{1}{N}. \tag{7}$$

A finite-size analysis shows that upon increasing the ribbon width, the gap narrows for any bulk disorder $\gamma_b$. In contrast, for edge disorder we observe a nonmonotonic behavior that can be explained by the competition of two effects: increasing the width of the GNR on one hand weakens the influence of the disorder as the ratio of edge to bulk sites decreases. An increasing number of lattice sites, on the other hand, reduces the finite-size effects and closes the gap. Thus, for $\gamma_e \gtrsim 2\bar{t}$, the gap first broadens when the GNR width is increased and then converges to the gap size of the ordered system, which finally vanishes in the limit $N_a \to \infty$. Similar studies for a different type of edge disorder, in which sites are randomly removed from the ribbon edges, can be found in the literature.[18,20,21]

To get further insight into the nature of the eigenstates of GNRs and substantiate our conclusions about their localization properties, we show the LDOS in the band center in Fig. 3. The magnifying inset for the ordered case shows the alternating structure of the edge states which are distinctive for the band center of zigzag GNRs.[28] In the presence of weak edge disorder, the checkerboard structure of the amplitudes persists in the bulk, while near the edges regions with significantly enhanced amplitudes emerge. The $A$-$B$ sublattice structure is no longer present for larger $\gamma_e$ as can be seen in the lower inset of Fig. 3. Here, the sites with vanishing amplitudes form a filamentary network in the bulk caused by the influence of the disordered edges. For bulk disorder, localization arises first near the edges of the system in the case of weak disorder, while localized states in the bulk of the GNR occur only for strong disorder. Varying the aspect ratio of the GNRs (right column of Fig. 3), we may tune the relative importance of the edges in the system. Although this effect is most pronounced for edge disorder, we observe also for bulk disorder such a "renormalization" of the disorder strength. A given $\gamma_{b,e}$ causes stronger localization for narrow GNRs.

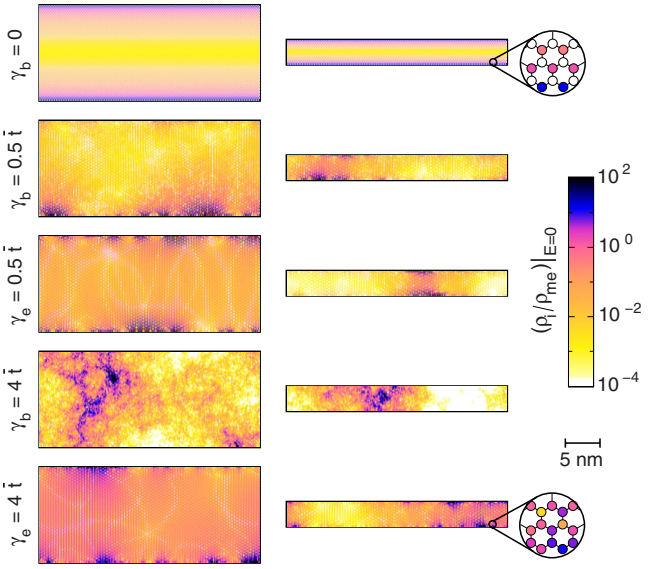


FIG. 3. (Color online) Normalized LDOS at the band center $(\rho_i/\rho_{\mathrm{me}})|_{E=0}$ for particular zigzag GNRs. In addition to contrasting bulk and edge disorder, we compare in the left (right) column the influence of the aspect ratios $L\times W=31.4\times 13.5(31.4\times 3.3)$ nm$^2$, corresponding to $256\times 64(256\times 16)$ sites. Results obtained by exact diagonalization.

### B. Time evolution of the wave function

Figure 4 shows the time evolution of an initially localized state, as calculated by the Chebyshev method.[27] The dynamics of the initial wave packet is characterized by a fast spreading process ($t \lesssim 10^3 t_0$), after which its extension does

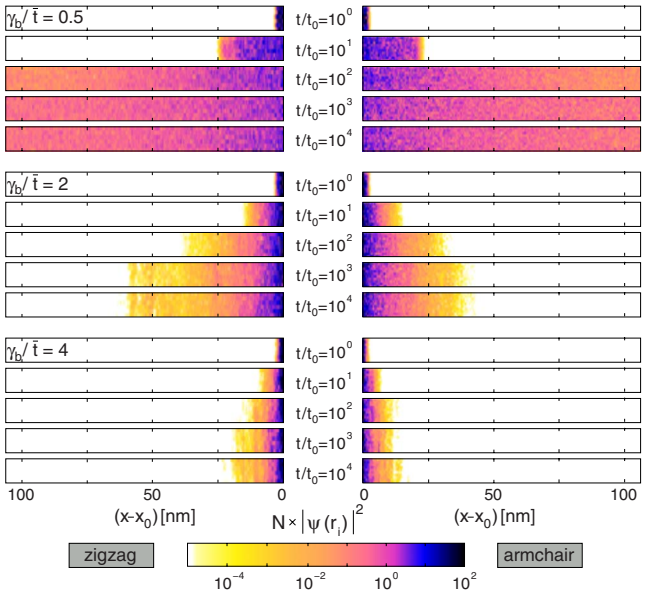


FIG. 4. (Color online) Time evolution of the normalized particle density $N|\psi(\mathbf{r}_i)|^2$ on disordered GRNs with zigzag and armchair geometries for different values of bulk disorder $\gamma_b$. Device dimensions: $(1.1\times 213)$ nm$^2$ corresponding to $6\times 1732$ atoms (zigzag) and $10\times 1000$ atoms (armchair). Times are measured in units of the inverse hopping element $t_0=1/\bar{t}$.

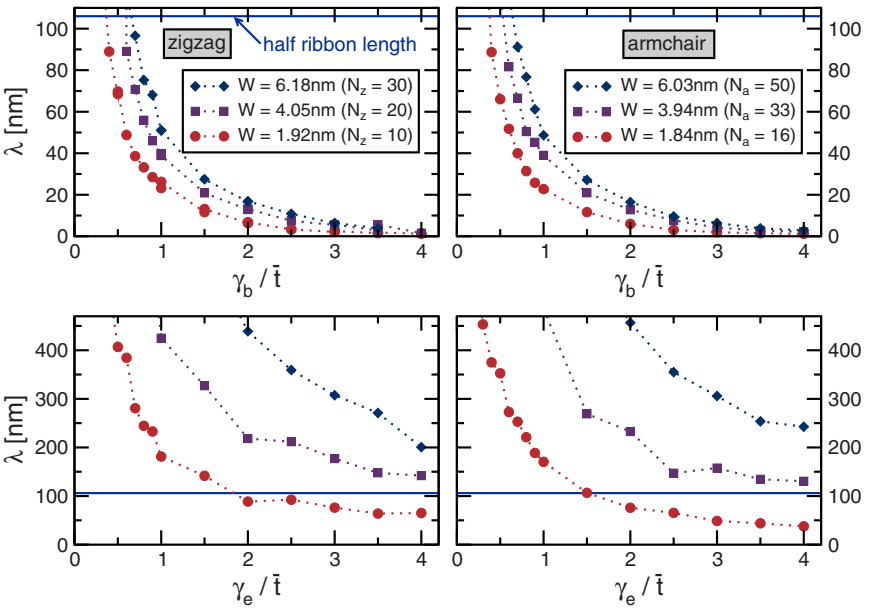


FIG. 5. (Color online) Localization length in dependence on bulk ($\gamma_b$) and edge ($\gamma_e$) disorder strength for armchair and zigzag GNRs. The values are sample averages obtained for ten GNRs of $L=213$ nm when the state has become quasistationary.

not change anymore, even for very long times. Clearly, on individual sites the amplitudes fluctuate in time; but the overall nature of the state for $t=10^4 t_0$ is quasistationary. The localization properties depend on both disorder strength and edge geometry. Obviously, armchair GNRs are more susceptible to the presence of disorder than those of zigzag type. For the shown GNRs of moderate length and weak disorder ($\gamma_{b,e}/\bar{t}=0.5$), the localization length is larger than the system size and thus the GNR is "metallic."

The extraction and quantitative discussion of the localization length in narrow GNRs is challenging. There is no problem to determine λ from an exponential fit

$$|\psi(\mathbf{r}_i)|^2 = |\psi(\mathbf{r}_0)|^2 \exp\left(-\frac{|\mathbf{r}_i - \mathbf{r}_0|}{\lambda}\right) \tag{8}$$

for a given initial state and disorder realization at any fixed time. But the such-determined λ strongly fluctuates, both in time and as a function of the chosen initial state and disorder realization. The temporal fluctuations of about 5–10 % can be eliminated by time averaging. Varying the initial state and/or comparing different disorder realizations leads to additional uncertainties of about 10–20 %. Therefore, we show in Fig. 5 sample averages over several combinations of initial states and disorder realizations.

Figure 5 indicates that the influence of the boundary (armchair/zigzag) is only of minor importance for the localization length. But we observe a pronounced difference between bulk and edge disorder, with $\lambda > L$ also for large values of $\gamma_e$ for most ribbon widths. For any fixed disorder strength, a decreasing width of the GNR systematically reduces λ since the influence of the lateral dimension is weakened and the system approaches the 1D limit. Values of λ which are significantly larger than half the system size (blue solid line) have to be taken with care since a reliable determination of the localization length requires $\lambda \lesssim L$. Clearly, the precise value of λ in those cases is of minor importance due to the metallic behavior of such finite GNRs. A quantitative comparison of the obtained localization lengths with estimates based on other methods[15–17] suffers from the different investigated disorder models. Nevertheless, the orders of magnitude match and the general tendencies are reproduced. The impact of disorder increases with decreasing ribbon width and the boundary type does not influence the localization length significantly for strong disorder. The pronounced dependence of the localization length on the ribbon type (armchair or zigzag) for the weakly disordered case reported in Refs. 15 and 16 is absent in our data. We attribute this to the different disorder models used.

## IV. SUMMARY

To conclude, Anderson localization takes place in disordered quasi-1D graphene nanoribbons but taking into account the actual device dimensions GNRs can be conducting at weak disorder strengths. This has been proven by calculating the localization length and time evolution of single-particle states. Within the local distribution approach, Anderson localization is identified by a log-normal distribution of the LDOS that shifts toward zero for increasing system size. The LDOS is directly measurable by scanning tunneling spectroscopy and therefore allows for a direct comparison of theory and experiment.

## ACKNOWLEDGMENTS

This work was funded by the Deutsche Forschungsgemeinschaft through the Research Program SFB TR 24 and the Competence Network for Technical/Scientific High-Performance Computing in Bavaria (KONWIHR). The numerical calculations have been performed on the TERAFLOP compute cluster at the Institute of Physics, Greifswald University.

[1] P. A. Lee and T. V. Ramakrishnan, Rev. Mod. Phys. **57**, 287 (1985).
[2] P. M. Ostrovsky, I. V. Gornyi, and A. D. Mirlin, Phys. Rev. B **74**, 235443 (2006).
[3] K. Nomura, M. Koshino, and S. Ryu, Phys. Rev. Lett. **99**, 146806 (2007).
[4] J. H. Bardarson, J. Tworzydło, P. W. Brouwer, and C. W. J. Beenakker, Phys. Rev. Lett. **99**, 106801 (2007).
[5] H. Schomerus, M. Titov, P. W. Brouwer, and C. W. J. Beenakker, Phys. Rev. B **65**, 121101(R) (2002).
[6] A. D. Mirlin, Phys. Rep. **326**, 259 (2000).
[7] A. Alvermann and H. Fehske, Eur. Phys. J. B **48**, 295 (2005); A. Alvermann and H. Fehske, Lect. Notes Phys. **739**, 505 (2008).
[8] Y. Niimi, H. Kambara, and H. Fukuyama, Phys. Rev. Lett. **102**, 026803 (2009).
[9] Y. Niimi, H. Kambara, T. Matsui, D. Yoshioka, and H. Fukuyama, Phys. Rev. Lett. **97**, 236804 (2006).
[10] T. Matsui, H. Kambara, Y. Niimi, K. Tagami, M. Tsukada, and H. Fukuyama, Phys. Rev. Lett. **94**, 226403 (2005).
[11] M. Morgenstern, J. Klijn, C. Meyer, and R. Wiesendanger, Phys. Rev. Lett. **90**, 056804 (2003).
[12] P. R. Wallace, Phys. Rev. **71**, 622 (1947).
[13] A. Quandt, C. Özdogan, J. Kunstmann, and H. Fehske, Nanotechnology **19**, 335707 (2008).
[14] A. Cresti, N. Nemec, B. Biel, G. Niebler, F. Triozon, G. Cuniberti, and S. Roche, Nano Res. **1**, 361 (2008).
[15] D. A. Areshkin, D. Gunlycke, and C. T. White, Nano Lett. **7**, 204 (2007).
[16] A. Lherbier, B. Biel, Y.-M. Niquet, and S. Roche, Phys. Rev. Lett. **100**, 036803 (2008).
[17] N. Nemec, K. Richter, and G. Cuniberti, New J. Phys. **10**, 065014 (2008).
[18] D. Querlioz, Y. Apertet, A. Valentin, K. Huet, A. Bournel, S. Galdin-Retailleau, and P. Dollfus, Appl. Phys. Lett. **92**, 042108 (2008).
[19] T. C. Li and S.-P. Lu, Phys. Rev. B **77**, 085408 (2008).
[20] M. Evaldsson, I. V. Zozoulenko, H. Xu, and T. Heinzel, Phys. Rev. B **78**, 161407(R) (2008).
[21] E. R. Mucciolo, A. H. Castro Neto, and C. H. Lewenkopf, Phys. Rev. B **79**, 075407 (2009).
[22] F. Tseng, D. Unluer, K. Holcomb, M. R. Stan, and A. W. Ghosh arXiv:0904.2116 (unpublished).
[23] P. W. Anderson, Phys. Rev. **109**, 1492 (1958).
[24] G. Schubert, A. Weiße, G. Wellein, and H. Fehske, in *High Performance Computing in Science and Engineering, Garching 2004*, edited by A. Bode and F. Durst (Springer-Verlag, Berlin, Heidelberg, 2005), pp. 237–250.
[25] B. Kramer and A. Mac Kinnon, Rep. Prog. Phys. **56**, 1469 (1993).
[26] H. Tal-Ezer and R. Kosloff, J. Chem. Phys. **81**, 3967 (1984).
[27] A. Weiße and H. Fehske, Lect. Notes Phys. **739**, 545 (2008); G. Schubert and H. Fehske, Phys. Rev. B **77**, 245130 (2008); H. Fehske, J. Schleede, G. Schubert, G. Wellein, V. S. Filinov, and A. R. Bishop, Phys. Lett. A **373**, 2182 (2009).
[28] K. Nakada, M. Fujita, G. Dresselhaus, and M. S. Dresselhaus, Phys. Rev. B **54**, 17954 (1996).
[29] S. Reich, J. Maultzsch, C. Thomsen, and P. Ordejón, Phys. Rev. B **66**, 035412 (2002); Y.-W. Son, M. L. Cohen, and S. G. Louie, Phys. Rev. Lett. **97**, 216803 (2006).